Ordered Porous Gold Electrodes to Enhance the Sensitivity of Enzyme-Based Glucose Sensors

Michael T.Y. Paul[†], Brandy Kinkead[†] and Byron D. Gates[†,*]

[†] Department of Chemistry and 4D LABS, Simon Fraser University, 8888 University Drive Burnaby, BC, V5A 1S6, Canada
* To whom correspondence should be addressed. Email: bgates@sfu.ca Tel: (+1) 778-782-8066; Fax: (+1) 778-782-3765

Glucose sensors are essential tools for diabetes patients to use in monitoring their blood glucose levels. However, to be able to detect glucose in non-invasively collected physiological fluids, such as tears and urine, the sensitivity of these glucose sensors must be significantly higher than sensors that are currently used to detect glucose concentrations in blood. Increasing the specific surface area of enzyme-based glucose sensors through the use of ordered porous gold electrodes has been shown to enhance the sensitivity of these sensors. The enzyme-based ordered porous gold glucose sensor was demonstrated to be suitable in detecting glucose concentrations ranges that are similar to those occurring in tears. Although sensitivity of the glucose sensor is enhanced, the saturation threshold of the sensor is lowered. Further optimizations of the porous gold electrodes are required to eliminate signal saturation of these improved sensors.

1. Introduction

Diabetes mellitus patients must monitor their blood glucose levels several times a day to maintain their proper health (1). Therefore, researchers around the world are constantly working to develop faster, simpler, and more accurate glucose sensing technologies. Out of the many glucose sensing technologies, enzyme-based electrochemical glucose sensors have proven to show excellent selectivity and sensitivity (2-4). The detection of glucose in non-invasively collected physiological fluids, such as tears and urine, requires further enhanced sensitivity to glucose than for sensors that are used to detect glucose concentration in blood (5-7). A method of increasing the efficiency and sensitivity of enzyme-based glucose sensors is to increase the surface roughness of the electrode material, which would allow a greater amount of enzyme to be adsorbed onto the electrode surfaces (8). Among the many possible electrode materials, gold has been commonly used in the preparation of biosensor electrodes due to its chemical stability, excellent conductivity, and affinity to biological molecules such as glucose oxidase (9-11). Many recent studies have demonstrated the use of nanoporous gold electrode materials to drastically improve the sensitivity of enzyme-mediated electrochemical glucose detection (12). The structural morphologies of these various nanoporous gold materials can include, but are not limited to, electrodeposited gold raspberry-like nanoparticles (13), electrodeposited gold nanowire array (14), dealloyed nanoporous gold (15), gold nanoparticle integrated carbon-

nanotube array (16), nanoporous black gold (17), and electrodeposited gold nanocoral (18). We have previously reported a method in preparing inverse opal films that have regular porosities (19) through the use of polystyrene (PS) sacrificial templates (20). In the study reported herein, we demonstrate a facile method for preparing nanoporous gold films from similar PS templates. To demonstrate the increased structural surface areas of these nanoporous gold electrodes, the gold films were used as a working electrode with adsorbed glucose oxidase in the electrochemical measurement of dissolved glucose in a physiological buffered saline (PBS).

2. Materials and Methods

2.1 Preparation of ordered porous gold electrodes

PS templates, as described in our previous publications (19,20), were used in the preparation of ordered porous gold electrodes (Au-OP electrodes). The general outline of the preparation was as follows: 1) gold nanoparticles (AuNPs) (13-nm in diameter) were decorated onto the surfaces of amino functionalized PS colloids (Polysciences Inc., 180-nm hydrodynamic diameter); 2) the decorated templates were mixed with excess AuNPs; 3) the solution of AuNPs and decorated PS colloids were drop cast into a circular well created by a hole (prepared using a hole-punch) in a polydimethylsiloxane (PDMS) film on top of a gold coated silicon substrate [gold film prepared as per (7)]; 4) the solution was allowed to evaporate at room temperature, promoting self-assembly of the PS particles (20); 5) the PDMS was peeled away from the gold coated substrate, revealing a dried film of PS templates and AuNPs; 6) the substrate was heated at 350°C to promote thermal degradation of the PS templates and annealing of AuNPs to form a continuous, porous matrix (Figure 1 a, inset); 7) the gold coated substrate was covered with another film of PDMS leaving one edge open for electric connection and a circular opening over the ordered porous gold film. This circular opening created a well-defined area for contact with the electrochemical analyte solution. A planar gold electrode was also prepared using similar procedures, but without the use of the modular template or the AuNPs, to serve as a control for comparison studies. The Au-OP electrodes had an average pore size of ~105 nm (Figure 1).

2.2 Physical Characterization

Scanning electron microscopy (SEM) was used to verify the formation of the porous gold film and the dimensions of the pores therein. Electron microscopy images and energy dispersive X-ray spectroscopy (EDS) data were collected using an FEI Strata™ Dualbeam™ (SEM/FIB) system operating at 12 kV.

2.3 Electrochemistry Characterization

Cyclic voltammetry (CV) experiments were performed using a Pine Instrument AFCBP1 Bipotentiostat with Pinechem® data analysis software. The prepared electrodes were incorporated as the working electrode into a typical three electrode setup using a Fisher accumet® epoxy body, single junction, 10-mm diameter Ag/AgCl reference electrode, along

with a Pt wire counter electrode. The CV analysis was performed after immersing the electrodes into a 10 mM PBS. These measurements were performed at a scan rate of 100 mV/s, and a sweep range from -400 to 750 mV for increasing glucose concentrations. Glucose concentrations were increased in increments of 0.1 mM between 0.1 to 0.5 mM, and increments of 1 mM from 1 to 8 mM. Control experiments were performed with planar gold electrodes. A calibration curve of the total charge generated from each measurement was constructed by integrating the area under each CV curve from 150 to 750 mV. Each measurement was performed with both a porous gold electrode and a planar gold electrode. Each of these electrodes had identical lateral dimensions and was prepared in a similar fashion. All gold electrodes were cleaned prior to enzyme incubation. The cleaning process involved treatment with an air based plasma (18 W for 30 s), followed by immersion in a Piranha solution (7:2 / H_2SO_4:H_2O_2 / v:v) for 2 min, and subsequently rinsed with 18 MΩ water and immersed in a 10% HCl (v:v) aqueous solution. Finally, the sample was carefully rinsed twice with 50 mL of 18 MΩ water before use. This process improved the hydrophilic properties of the electrode and removed organic and oxide contaminants from the electrode surfaces.

3. Results and Discussion

3.1 Surface area determination

Cyclic voltammetry was used to assess the active electrochemical surface area (ECSA) of the respective electrodes (porous and planar electrodes). The area under the oxide reduction peak was used to calculate the surface area, assuming the reduction of a monolayer of gold oxide on the electrode surface is ~386 μC/cm^2 (21). Gold oxide was formed over the surfaces of the electrode by incubating the electrodes in a mixture of concentrated sulfuric acid and 30 % hydrogen peroxide solution (7:3; v/v) for 30 seconds prior to PDMS encapsulation. CV scans were acquired in the PBS electrolyte and the resulting Au oxide reduction peak analyzed to determine ECSA (data not shown). Using this method, it was determined that the Au-OP electrodes had nearly 28 times as much surface area as the planar electrode. The roughness factor of the planar gold electrode and Au-OP electrodes were 1.27 and 36, respectively. This roughness factor for the Au-OP electrodes is within a reasonable range of other types of porous electrode structures (9-18,22).

3.2 Glucose sensing with glutaraldehyde fixed glucose oxidase

The electrode surfaces were modified with glucose oxidase (GOx) in order to detect dissolved glucose in solution. The immobilization of GOx enzyme was achieved by mixing a solution of GOx (3 g/mL) with glutaraldehyde, a common fixative for biomolecules, (in a 1:1 concentration ratio), and incubating the electrodes in this solution overnight. The electrochemical analyses of these electrodes were performed after extensive rinsing with deionized water (>50 mL, three times). In this analysis, the glucose oxidation peak occurred at ~425 mV (Figure 2). A slight broadening of the glucose oxidation peak was observed in the CV scans acquired at 100 mV/s (Figure 2a). This observation suggests that the mass transport of reactants and by-products

within the porous structure are rather slow (3). This observation is in agreement with the results obtained at 50 mV/s scan rates, where mass transport limitations are less significant and more well-defined glucose oxidation peaks are observed (Figure 2b). Furthermore, control experiments performed with planar gold electrodes failed to exhibit any measurable GOx activities below the glucose concentration of 3 mM. The use of glutaraldehyde was shown to improve the sensitivities of biosensor by crosslinking and adsorbing enzymes onto materials that have less affinity toward biological molecules (22). However, it was reported that excess glutaraldehyde trapped GOx, or excess glutaraldehyde to GOx ratio can cause an overall decrease in sensitivity (23). We suspect that the decrease in activities we observed for the planar gold electrode may be caused by an excess presence of glutaraldehyde on the gold surfaces.

3.3 Glucose sensing with glucose oxidase

In order to increase the GOx activities for the planar gold and Au-OP electrodes, the same experiments were performed again with electrodes that were incubated in a solution containing only GOx (3 g/mL) without the presence of glutaraldehyde. The CV scans resulting from this preparation demonstrated a much higher current (Figure 3 a,b) in comparison to the results obtained with electrodes containing the glutaraldehyde fixed GOx. However, the electrochemical responses of the Au-OP electrodes are mass transport limited, which can be observed in the CV scans where the peaks are ill-defined and maintained a relatively constant rate of increasing current with applied potential. This phenomenon was also reported in a previous study that suggested this transport limitation was due to the inhibition of the GOx, caused by the relatively large amounts of locally generated hydrogen peroxide from the GOx (14). Calibration curves of the total charge generated from each measurement were constructed by integrating the area under each CV scan from 150 to 750 mV. The total charge generated by the ordered porous gold electrodes was approximately twice that of its planar counterpart (Figure 3 c). The electrochemical signal generated by the Au-OP electrodes may, however, be underestimated due to skewed baselines.

In subsequent electrochemical analyses, we held the experimental conditions constant except that we lowered the CV scan rate to 50 mV/s (Figure 4). This decrease in scan rate allowed more time for the analyte to equilibrate with the porous structure in order to compensate for the mass transport limited phenomenon observed for the Au-OP electrodes (Figure 4a). The slower scan rate, however, decreased the signal of the planar gold electrodes to baseline levels due to the reduced electron flux at the electrode surfaces (Figure 4b). The total charge generated by the ordered porous gold electrode was ~50 times larger than its planar counterpart (Figure 4 c). It is also possible that the total charge generated by the planar gold electrode was under estimated in this analysis due to the system's limitation in detecting diminished currents.

Overall, without glutaraldehyde the catalytic peak current is linearly proportional to glucose concentrations from 0.1 to 0.5 mM at a scan rate of 50 mV/s with a correlation coefficient of 0.991. The sensitivity and limit of detection for the ordered porous electrodes at a scan rate of 50 mV/s are 21.14 $\mu A\ mM^{-1}\ cm^{-2}$ and 0.073 mM, respectively. The detection limit was calculated as $k\sigma_b/m$, where σ_b is the standard deviation of the background current, m is the slope of the linear part of the calibration curve, and with a k value of 3 to achieve a confidence level of 99.86%. The sensitivities of these porous gold electrodes is higher than that observed for arrays of gold nanoparticle modified nanotubes (1.13$\mu A\ mM^{-1}\ cm^{-2}$) (16) and arrays of gold nanowires

(15.1μA mM^{-1} cm^{-2}) (14), and is comparable to the reported sensitivity of gold nanocorals (22.6 μA mM^{-1} cm^{-2}) (18). Furthermore, the linear range and detection limits of our Au-OP electrodes are suitable for detecting glucose concentrations in tears where the reported glucose concentration in tears is ~0.3 mM in healthy adults (5). The detection limit of these Au-OP electrodes is higher than that for the gold nanocorals (10 μM) (18). This increase in detection limit may be attributed to the mass transport difficulties we observed for the Au-OP films (i.e. peak broadening, and a skewed baseline). Therefore, further optimization of these Au-OP electrodes is still required.

4. Outlook

We have demonstrated that Au-OP electrodes can be used in detecting very low concentrations of glucose. The electrochemical signals generated with the Au-OP electrodes with GOx are at least twice as much as that for a planar Au electrode. However, due to the large amount of adsorbed GOx on the Au-OP electrode surfaces, a saturation effect was observed possibly due to a significantly larger amount of hydrogen peroxide produced by the increased levels of GOx within the porous electrodes. Amperometric measurements may also be used to avoid this saturation problem that was observed for our voltammetric detection method (25). In amperometric based detection, the dissolved glucose within the pores will be oxidized simultaneously during the applied potential (25). The corresponding peak current can be correlated to glucose concentrations within the pores, and the diffusion limited Cottrell current will not play an important role in the detection of glucose. Additional charge carriers, such as flavin adenine dinucleotide (FAD), can be used in conjunction with GOx, to minimize the production of hydrogen peroxide and to produce sharper, more well-defined peaks (26, 27). Finally, a GOx activity interference study (e.g., GOx activity determined in the presence of ascorbic acid, uric acid, or bovine serum albumin) can be performed to determine if these Au-OP electrodes are suitable for the detection of glucose concentrations in biological fluids, such as tears and urine samples.

5. Conclusions

In summary, we demonstrated the use of Au-OP electrodes, with adsorbed GOx, to enhance the sensitivity of measuring dissolved glucose concentrations. The increased surface area of the Au-OP electrodes was shown to enhance sensitivity and the detection limit to dissolved glucose when compared to planar Au electrodes. The increased specific surface area of the Au-OP electrodes facilitates a high loading of GOx on the electrode surfaces. This increased loading of GOx on the surfaces of the electrodes enhanced their sensitivity and detection limit for measuring glucose, but this saturation with GOx also lowered the saturation threshold for detection. The use of Au-OP electrodes in GOx based, voltammetric glucose sensors requires further optimization, and an amperometric method of detecting glucose may overcome this saturation limitation. Further enzymatic modification of the Au-OP electrodes may also be ideal to optimize the use of Au-OP electrodes in GOx-based glucose sensors.

Acknowledgments

This work was supported in part by the Natural Sciences and Engineering Research Council (NSERC) of Canada and the Canada Research Chairs Program (B.D. Gates). This work made use of 4D LABS shared facilities supported by the Canada Foundation for Innovation (CFI), British Columbia Knowledge Development Fund (BCKDF), Western Economic Diversification Canada, and Simon Fraser University.

References

(1) K. Alberti; P. Z. Zimmet, *Diabetic Med.*, **15**, 539 (1998).
(2) M.L. Cortez, G.A. Gonzalez, F. Battaglini, *Electroanalysis*, **23**, 156 (2011).
(3) S. Ferri; K. Kojima; K. Sode, *Journal of Diabetes Science and Technology*, **5**, 1068 (2011).
(4) J. N. Patel; B. Kaminska; B. Gray; B. D. Gates, *14th IEEE International Conference on Electronics, Circuits and Systems*, (2007).
(5) J. T. Baca; D. N. Finegold; S. A. Asher, *Ocular Surface*, **5**, 280 (2007).
(6) C. R. Taormina; J. T. Baca; S. A. Asher; J. J. Grabowski; D. N. Finegold, *J. Amer. Soc. Mass Spectr.*, **18**, 332 (2007).
(7) J. N. Patel; B. Gray; B. Kaminska; B. Gates, *Canadian Conference on Electrical and Computer Engineering*, 421 (2007).
(8) Y. Myung; D. M. Jang; Y. J. Cho; H. S. Kim; J. Park; J. U. Kim; Y. Choi; C. J. Lee, *J. Phys. Chem. C*, **113**, 1251 (2009).
(9) S. Ernst; J. Heitbaum; C. H. Hamann, *J. Electroanal. Chem.*, **100**, 173 (1979).
(10) K.B. Kokoh; J.M. Leger; B. Beden; C. Lamy, *Electrochim. Acta.*, **37**, 133 (1992).
(11) Y. Ling; J.C. Elkenbracht; W.F. Flanagan; B.D. Lichter, *J. Electrochem. Soc.*, **144**, 2689 (1997).
(12) T. Li; F. Jia; Y. Fan; Z. Ding; J. Yang, *Biosensors and Bioelectronics*, **42** 5-11 (2013).
(13) S. Manivannan; R. Ramaraj, *J. Nanopart. Res.*, **15**, 1978 (2013).
(14) X. Y. Zhang; D. Li; L. Bourgeois; H. T. Wang; P. A. Webley, *Chemphyschem*, **10**, 436 (2009).
(15) H. J. Qiu; L. Y. Xue; G. L. Ji; G. P. Zhou; X. R. Huang; Y. B. Qu; P. J. Gao, *Biosens. Bioelectron.*, **24**, 3014 (2009).
(16) Y. Zhou; S. Yang; Q. Qian; X. Xia, *Electrochem. Commun.*, **11**, 216-219 (2009)
(17) H. Jeong; J. Kim, *Electrochim. Acta*, **80**, 383 (2012)
(18) T. M. Cheng; T. K. Huang; H. K. Lin; S. P. Tung; Y. L. Chen; C. Y. Lee; H. T. Chiu, *ACS Appl. Mater. Interfaces*, **2**, 2773 (2010).
(19) B. Kinkead; J. van Drunen; M. T. Y. Paul; K. Dowling; G. Jerkiewicz; B. D. Gates, *Electrocatalysis*, **4**, 179 (2013).
(20) B. Gates; Y. Xia, *Adv. Mater.*, **13**, 1605 (2001).
(21) S. Trasatti; O. A. Petrii, *Pure Appl. Chem.*, **63**, 711 (1991).
(22) R. A. Sheldon, *Adv. Synth. Catal.*, ***349***, 1289-1307 (2007).
(23) J. L. House; E.M. Anderson; W. K. Ward; *J Diabetes Sci Technol.*, ***1***, 18-27 (2007).
(24) T. J. Li; F. L. Jia; Y. X. Fan; Z. F. Ding; J. Yang, *Biosens. Bioelectron.*, **42**, 5 (2013).
(25) J. Wang, *Chem. Rev.*, **108**, 814 (2008).
(26) S. Park; H. Boo; T. D. Chung, *Anal. Chim. Acta*, **556**, 46 (2006).
(27) M. Imamura; T. Haruyama; E. Kobatake; Y. Ikariyama; M. Aizawa, *Sensor Actuat. B-Chem*, **24**, 113 (1995).

Figure Captions

Figure 1. (a) Low magnification scanning electron microscopy (SEM) of porous (105-nm diameter pore size) gold electrode; inset: optical image of a round ($0.071 cm^2$) porous gold film prepared on top of gold coated silicon substrate. (b) High magnification SEM of the porous gold film with 105-nm diameter pores.

Figure 2. (a) CV scans performed at 100 mV/s with glutaraldehyde (GA) fixed glucose oxidase (GOx) ordered porous gold electrodes (105-nm diameter pores) for detecting glucose concentrations from 0.3 to 8 mM. (b) CV scans of the same electrode in (a), with CV performed at 50 mV/s.

Figure 3. (a) CV scans performed at 100 mV/s with GOx coated ordered porous gold electrodes for detecting glucose concentrations from 0.1 to 8 mM. (b) CV scans of a planar gold electrode coated with GOx for the detection of glucose while scanned at 100 mV/s. (c) Total charge accumulated by each electrode in (a) and (b) during glucose oxidation over a range of glucose concentrations.

Figure 4. (a) CV scans performed at 50 mV/s with GOx coated ordered porous gold electrodes for the analysis of glucose concentrations from 0.1 mM to 2 mM. (b) CV scans of a planar gold electrode decorated with GOx also acquired at 50 mV/s. (c) Total charge generated by each electrode in (a) and (b) at different glucose concentrations.

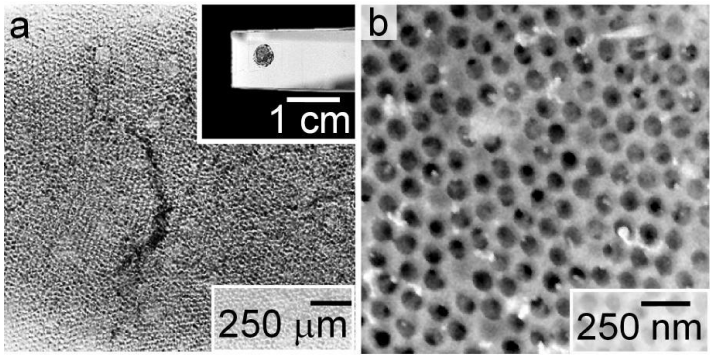

Figure 1. (a) Low magnification scanning electron microscopy (SEM) of porous (105-nm diameter pore size) gold electrode; inset: optical image of a round ($0.071 cm^2$) porous gold film prepared on top of gold coated silicon substrate. (b) High magnification SEM of the porous gold film with 105-nm diameter pores.

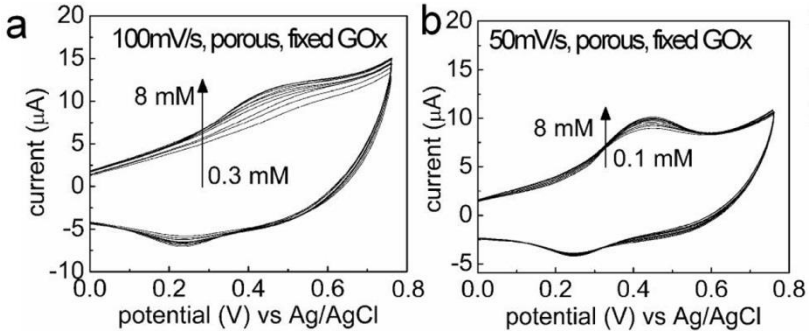

Figure 2. (a) CV scans performed at 100 mV/s with glutaraldehyde (GA) fixed glucose oxidase (GOx) ordered porous gold electrodes (105-nm diameter pores) for detecting glucose concentrations from 0.3 to 8 mM. (b) CV scans of the same electrode in (a), with CV performed at 50 mV/s.

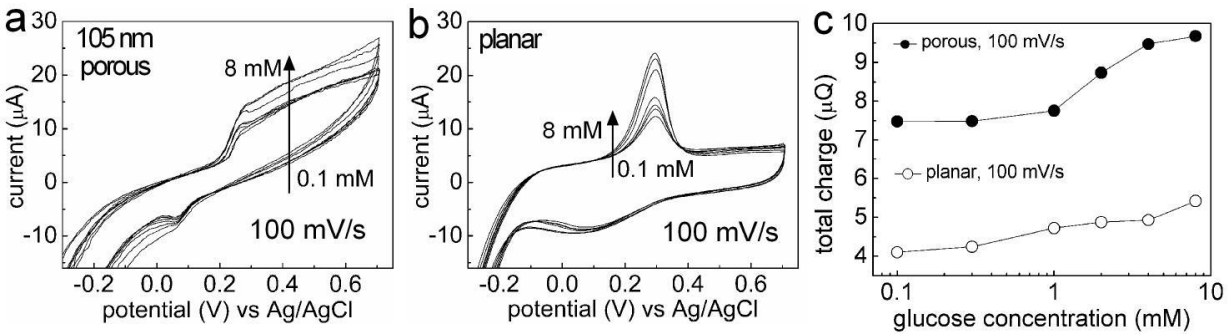

Figure 3. (a) CV scans performed at 100 mV/s with GOx coated ordered porous gold electrodes for detecting glucose concentrations from 0.1 to 8 mM. (b) CV scans of a planar gold electrode coated with GOx for the detection of glucose while scanned at 100 mV/s. (c) Total charge accumulated by each electrode in (a) and (b) during glucose oxidation over a range of glucose concentrations.

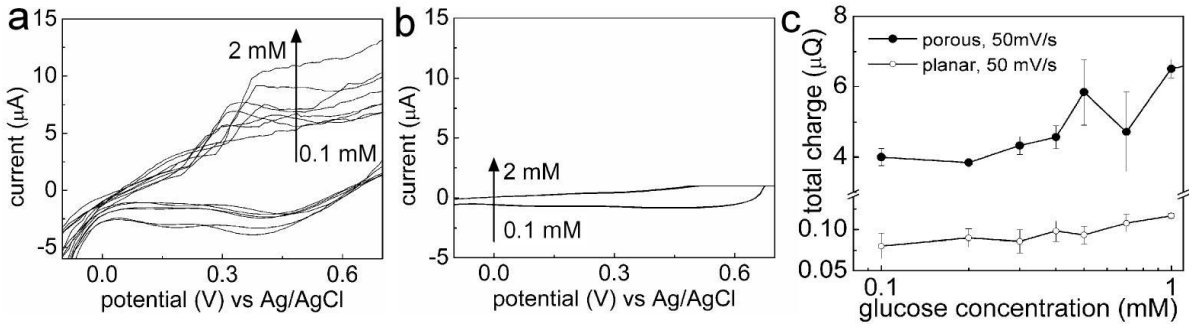

Figure 4. (a) CV scans performed at 50 mV/s with GOx coated ordered porous gold electrodes for the analysis of glucose concentrations from 0.1 mM to 2 mM. (b) CV scans of a planar gold electrode decorated with GOx also acquired at 50 mV/s. (c) Total charge generated by each electrode in (a) and (b) at different glucose concentrations.